Pamukkale Univ Muh Bilim Derg, 28(7), 977-986, 2022

Pamukkale Üniversitesi Mühendislik Bilimleri Dergisi

Pamukkale University Journal of Engineering Sciences

Experimental performances of nonlinear GPC and discrete-time PID in multivariate process: NARIMAX and ARX models in temperature control of reactive distillation column in synthesis of biodiesel from waste cooking oil

Çok değişkenli proseste doğrusal olmayan GPC ve kesikli-zaman PID'nin deneysel performansı: Atık yemeklik yağdan biyodizel sentezinde tepkimeli damıtma kolonunun sıcaklık kontrolünde NARIMAX ve ARX modelleri

Mehmet Tuncay ÇAĞATAY[1*], *Süleyman KARACAN*[2]

[1]Ministry of National Defense, General Directorate of Technical Services, Ankara, Turkey.
mehmetcagatay71@gmail.com
[2]Department of Chemical Engineering, Faculty of Engineering, Ankara University, Ankara, Turkey.
karacan@eng.ankara.edu.tr

Received/Geliş Tarihi: 03.03.2022 Revision/Düzeltme Tarihi: 09.06.2022 doi: 10.5505/pajes.2022.75570
Accepted/Kabul Tarihi: 27.06.2022 Research Article/Araştırma Makalesi

Abstract

Generalized Predictive Control (GPC) is a popular Model Predictive Control algorithm that has the advantage of effectively managing the multivariate process. In this study, experimental temperature control of the reactive distillation column process in calcium–oxide catalyzed biodiesel synthesis from waste cooking oil was investigated using nonlinear GPC based on NARIMAX model and discrete time PID control based on ARX model. Before the experiments, the effects of all parameters on temperature and biodiesel mole fraction were analyzed by HYSYS simulation. Afterwards, control studies were carried out with the help of WCO flow rate and reboiler heat duty manipulating variables and algorithms and codes developed in MATLAB. In the SISO experiments, significant convergent temperature responses were obtained in each region controlled by the relevant manipulating variable. Regarding MIMO experiments, all proposed methods except the non-decoupled nonlinear GPC were found to converge ultimately to their setpoints, but the best performance was achieved in decoupled nonlinear GPC with less severe interaction, smaller settling time, no oscillations and lower IAE and ISE.

Keywords: Generalized predictive control, PID control, Multivariable control, Reactive distillation column, Biodiesel, Waste cooking oil.

Öz

Genelleştirilmiş Öngörülü Kontrol (GPC), çok değişkenli prosesi etkili bir şekilde kontrol edebilme avantajına sahip popüler bir Model Öngörülü Kontrol algoritmasıdır. Bu çalışmada, atık yemeklik yağdan kalsiyum-oksit katalizörlü biyodizel sentezinde tepkimeli damıtma kolonu prosesinin, NARIMAX model tabanlı doğrusal olmayan GPC ve ARX model tabanlı kesikli-zaman PID kontrol ile deneysel sıcaklık denetimi incelenmiştir. Deneyler öncesinde, tüm parametrelerin sıcaklık ve biyodizel mol kesri üzerine etkileri HYSYS simülasyonu ile analiz edilmiştir. Müteakiben, WCO akış hızı ve kazan ısı yükü ayar değişkenleri ve MATLAB'da geliştirilen algoritmalar ve kodlar yardımıyla denetim çalışmaları gerçekleştirilmiştir. SISO deneylerinde, ilgili ayar değişkeni ile kontrol edilen her bir bölgede önemli seviyede yakınsak sıcaklık cevapları elde edilmiştir. MIMO deneyler açısından ise, ayırımsız doğrusal olmayan GPC haricinde, önerilen tüm yöntemlerde en nihayetinde ayar noktalarına yakınsama olduğu tespit edilmiştir, ancak en iyi performans, daha az şiddetli etkileşime sahip, daha küçük yerleşme zamanlı, salınım göstermeyen ve daha düşük IAE ve ISE'ye sahip ayırımlı doğrusal olmayan GPC ile elde edilmiştir.

Anahtar kelimeler: Genelleştirilmiş öngörülü kontrol, PID kontrol, Çok değişkenli kontrol, Tepkimeli damıtma kolonu, Biyodizel, Atık yemeklik yağ.

1 Introduction

Petroleum diesel is widely used in internal combustion engines and causes greenhouse gas emissions and global warming. Biodiesel, which is an alternative to petroleum diesel, seems to be an effective measure against the increase in fossil fuel consumption due to the rapid growth of the global population and industrial development [1]. The major reason why it is not used as a large-scale fuel is its relatively higher cost compared to fossil-based diesel due to expensive raw materials and costly homogeneous conventional process [2].

To overcome the high cost of the raw material, economical and sustainable waste cooking oil (WCO) has been proposed due to its lower price and higher availability compared to pure refined vegetable oils such as palm oil, soybean and sunflower oil with extra processing costs [3]. Improper waste management and direct drainage of WCO from homes and restaurants can adversely affect human health, plant and aquatic life through water and soil pollution, leading to serious environmental problems and costly wastewater treatment. Its use as a raw material allows us to obtain both useful and economical biodiesel and eliminate its disposal as waste in landfills [4].

Synthesis of biodiesel with a homogeneous base catalyst has fast reaction rate, high yield, mild reaction conditions and less energy consumption. However it is sensitive to the free fatty acid (FFA) content (>2% by weight) in the oil, and soap and glycerol are formed as by-products. Therefore, the process needs more water during purification. On the other hand, although homogeneous acid catalysts are insensitive to both FFAs and the water content in the oil, they have disadvantages such as relatively slow reaction rate and corrosiveness, causing soap formation, difficulties in separating from the product and

*Corresponding author/Yazışılan Yazar

reusability. In brief, the homogeneous basic process produces a large amount of wastewater that must be treated before discharge, and also requires purification of the biodiesel by removing impurities, water, dissolved and no reusable homogeneous catalyst. As for the acid one, it causes corrosion and requires longer reaction times [5].

In terms of heterogeneous catalysts, the advantages can be summarized as easy separation, simple recovery techniques and reusability of the catalyst from the product. Even though catalyst preparation is relatively expensive, milder reaction conditions are needed and basic ones have a faster reaction rate than the homogeneous process. Also, formation of wastewater and its negative environmental effects can be prevented. That is, by reducing amount of equipment needed for purification, the steps are simplified and thus product purification becomes easier. Further, the catalyst can be easily separated from the reaction mixture, thus ensuring its reusability [5]. Generally, metal oxides, zeolites and hydrotalcites are used as heterogeneous basic catalysts and exhibit high catalytic activity [6]. Among them, calcium-oxide (CaO) has advantages such as higher basicity, lower solubility, higher availability, lower cost, milder reaction conditions and convenient reusability [7].

Another important issue affecting the cost is operating expenses. The traditional manufacturing process consists of many units and requires a high alcohol to oil molar ratio to complete the reaction. At this point, energy efficient technique, process intensification comes to the fore with factors such as low reaction time, product purification, and elimination of mass transfer resistance. Reactive Distillation (RD) is one of the important process intensification methods in using biodiesel production [8]. The cost-reducing factors in the RD process are the simultaneous reaction and separation, the ability to shift the equilibrium to the product side, the integration of heat, and the use of low-cost and uncomplicated constructions [9]. Wang et al. [10] showed 10% less energy consumption and 50% production increase in methyl acetate hydrolysis in the RD process compared to that produced with a fixed bed reactor. On the other hand, considering the complex interactions occurring in the reaction and vapor-liquid equilibrium, the nonlinearity of the process, the simultaneous occurrence of separations, and keeping the operating conditions, it is clear that the control of the RD column process with equilibrium reaction is essential.

Some simulation studies on process control of the distillation column can be summarized as follows. Alaei et al. [11] used HYSYS and compared ARX-based linear generalized generic model (GPC) with neural network-based nonlinear predictive control. Cong et al. [12] presented a model-based control strategy combining the nonlinear wave model with a generalized generic model control. Liu et al. [13] proposed a nonlinear MPC based on the wave model. Regalado-Méndez et al. [14] devised a plant-wide economic control strategy for biodiesel production. Cheng et al. [15] designed a time-delayed active disturbance rejection GPC strategy. Giwa et al. [16] implemented MATLAB/Simulink's MPC toolbox for renewable energy. Regarding the multivariable theoretical control, Wu [17] proposed an improved PID controller optimized with an extended non-minimal state space model based MPC, Saravanakumar et al. [18] used Lagrange-based state transition algorithm to tune the decentralized PID controller, using its numerical stability and performance, Abraham et al. [19] developed an optimal GPC using the first principle and linearized 16th order and reduced fifth order models, Hadian et al. [20] used an event-based neural network prediction controller using the Cuckoo Optimization Algorithm for the nonlinear process, Shin et al. [21] used HYSYS and examined an MPC integrated neural network model in the nonlinear process, and Cheng et al. [22] proposed a dynamic decoupling strategy based on active disturbance rejection control for a first order system with an observer based on a nonlinear wave model.

On the other hand, there are very few experimental studies on the process control of the distillation column containing the multivariate nonlinear system with the GPC algorithm. These studies can be summarized as follows. Regarding the separation of the methanol-water mixture in the packed distillation column, Karacan et al. [23] used the ARIMAX model and investigated optimal adaptive GPC, Hapoglu et al. [24] applied CARIMA-based GPC and DMC system based on nonparametric model and Karacan [25] applied Nonlinear Long Range Predictive Control with NARIMAX model. In terms of multivariable control, Mahfouf et al. [26] proposed GPC-based feed-forward Long Range Predictive Control using Takagi-Sugeno Kang piecewise fuzzy modeling, Karacan et al. [27] used the General Model Control structure based on a linear auto-recursive extensive and NARIMAX black box models, Marangoni et al. [28] proposed a method using PID control via static decoupling with distributed action, and Liu et al. [29] proposed an adaptive GPC strategy for the internal thermally coupled column. Haskerl et al. [30] described the application of economy of optimizing control to a multi-product pilot-plant scale RD process based on do-mpc, reducing computation times of NMPC. Recently, Yadav et al. [31] investigated a pilot-scale binary column using step input excitation for multiple input and output (MIMO) processes, where the mathematical model is considered a first-order plus dead-time structure.

Following the evaluation of the studies mentioned so far, the theoretical controls of the temperatures of reaction and reboiler sides of RD column process in biodiesel production from WCO with multivariable NARIMAX model-based nonlinear GPC and ARX model-based discrete-time PID control were investigated in our previous study [32] using algorithms and codes developed in MATLAB environment with and without decoupling. In the study, model's and control constants defining the heterogeneous CaO-packed RD column process were determined experimentally with the help of PRBS effects by total flow rate and reboiler heat duty manipulating variables. In nonlinear system, the powers of the manipulating variables were taken as the basis in definition of the nonlinearity, and decoupling was achieved for N steps ahead future time with the help of matrix solution using codes developed in MATLAB.

In this study, the experimental controls of the reaction and reboiler temperatures of the CaO-packed continuous flow and fully methanol-refluxed RD column process in biodiesel synthesis from WCO were investigated, and the experimental control performances were compared. In the experimental studies, model's and control constants defining the process and the codes developed in MATLAB for algorithms were taken as the same ones developed for our previous theoretical study [32] since the experimental control studies were carried out at the same process and operating conditions. Before starting the control studies, the process was simulated with Aspen HYSYS to examine the theoretical effects of the parameters on the temperature and biodiesel mole fraction of the reaction and the reboiler sides. In the light of knowledge mentioned so far, our study is considered as original since no experimental control study with nonlinear GPC of the multivariate RD column process in biodiesel synthesis was found in the literature.

2 Control system design

2.1 Experimental control methodology

Two–partitioned and heterogeneous CaO packed RD process with feed and product line and online control units is given as in Figure 1. Initially, a mixture of biodiesel and methanol with a total volume of 2025 ml was placed in the reboiler and the mantle heater was activated online. Thus, the process started with the heating of the mixture to the set value in the reboiler. The methanol vapor rising in the column condensed and flowed downwards when encountering the cooler environment. In this way, the temperature of the column increased over time while the methanol vapor rose upwards. When it reached the top of the column, it became liquid in the condenser and completely refluxed down the column. Thus, it was ensured that there was always excess methanol in the reaction zone. The process continued for some time, and the temperatures of the reaction, stripping and reboiler sections reached a steady state after nearly 40-50 min. Just then, the digital pumps were started online, and two different feed lines were sent separately to the top of the column at the desired WCO flow rate and the methanol flow rate providing desired mole ratio. These supply lines were previously heated to the inlet temperature with the help of heat exchangers and a circulating hot water bath, and then, they were combined with the help of a two-inlet and one-outlet connector, and fed from the top of the column as a single line. When the reactants and products reached the reboiler, the ball valve, added to the outlet line, was opened and the reboiler liquid level was tried to be kept constant at half the full rate.

Subsequently, the relevant control software with the algorithm prepared in the MATLAB environment was run for the related experiment. In single input and output (SISO) experiments, each process response was obtained separately by applying the relevant input only to the associated section. Then, it was aimed to bring the temperature response of the controlled section to the setpoint by changing the related manipulating variable. On the other hand, in MIMO experiments, the responses of all regions were read from each section simultaneously after each input was applied concurrently to the relevant part of the process. Thus, by changing the manipulating variables synchronously, it was aimed that the temperatures of both sides reach the setpoints at the same time. To do so, the system itself constantly read and recorded the temperatures with the help of thermocouples placed in RD column, calculated the signals of the manipulating variables and automatically sent them to the relevant controller units such as digital peristaltic pumps and mantle heater.

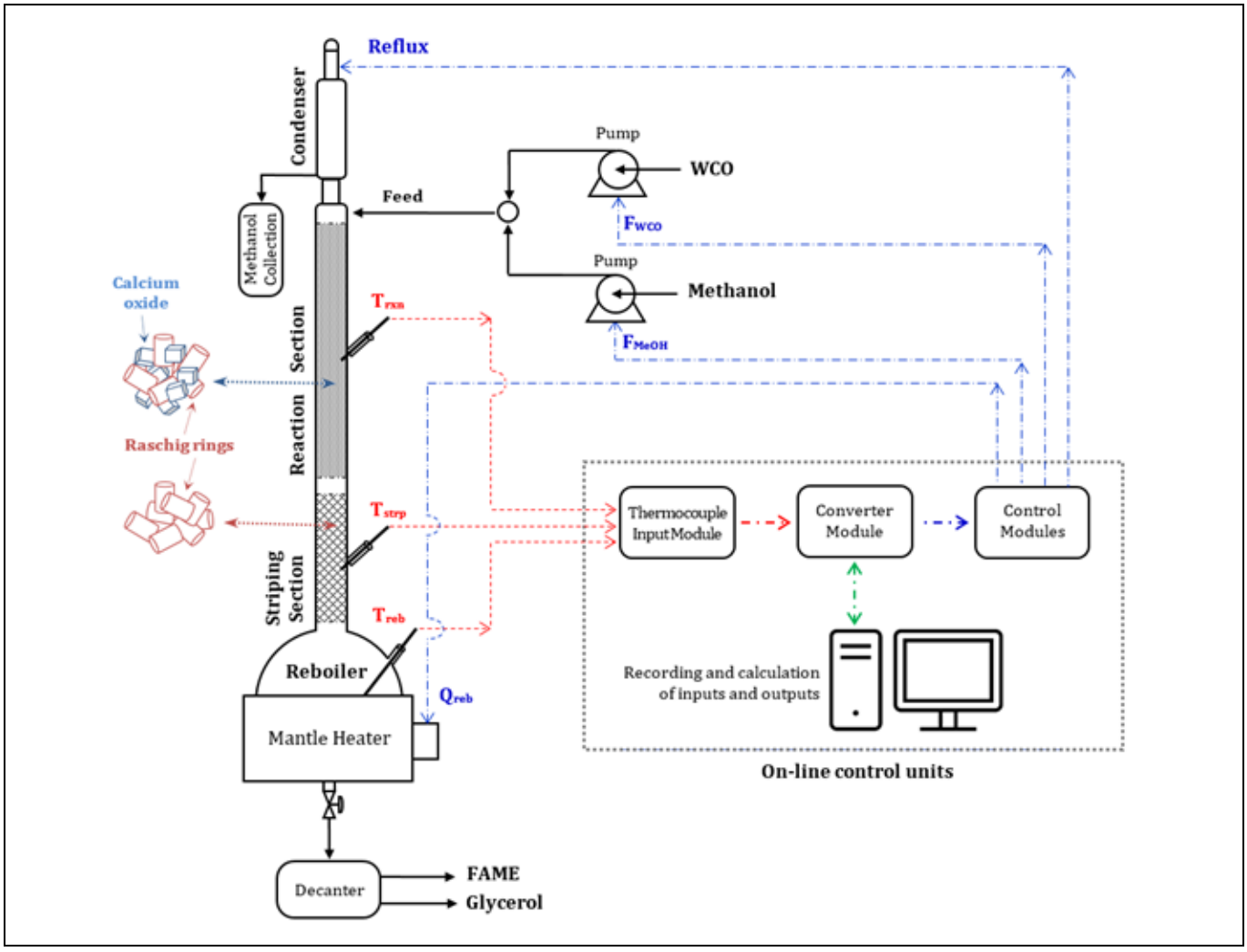

Figure 1. Schematic diagram of the process with online control units.

2.2 Simulation with Aspen HYSYS

Before the experimental control studies, theoretical effects of parameters such as feed inlet temperature, feed flow rate, mole ratio, reboiler heat duty and reflux ratio on temperature and biodiesel mole fraction were examined with the help of HYSYS simulation. Thus, it was aimed to determine which parameters have more effect on the process and to contribute to the determination of manipulating variables. In the simulation, the reaction type and kinetic parameters, the overall and intermediate steps of the transesterification reaction and the description of the process were taken as in [33],[34].

2.3 Control laws and constants

Since the control laws, model parameters and control constants to be used in experimental control studies are the same as those generated and used in our previous theoretical control study [32], the methods are not repeatedly explained here in detail to avoid duplication. Instead, this section has focused more on its experimental applications, as outlined below.

In the study, the exponential power of the manipulating variables $u(t)^m$ was based on the description of the nonlinear process and used in nonlinear GPC applications with NARIMAX model. Usually, the j step-ahead estimation of the response and the future input data is calculated using Equations (1)-(3), respectively, where f_j represents the free response of the process and G_j is the polynomial.

$$\bar{y}(t+j) = G_j \Delta u^m(t+j-1) + f_j \tag{1}$$

$$\Delta u^m = (G^T G + \lambda I)^{-1} G^T (r - f) \tag{2}$$

$$u^m(t) = u^m(t-1) + (G^T G + \lambda I)^{-1} G^T (r - f) \tag{3}$$

During the control with SISO NLGPC, the u^m obtained from the first element of the vector Δu^m, which contains the estimated solutions for j from 1 to N_u, is applied to the relevant section and a response is received. Regarding to control with MIMO NLGPC, the study was carried out in two categories, non-decoupled and decoupled algorithms. In the non-decoupled, Equations (4) and (5) can be written separately for each part. By solving these equations individually, the vectors Δu_1^m and Δu_2^m and the future values of the manipulated variables, u_1^m and u_2^m, are achieved. Then, the first term of these is applied to the process at time t, and responses are obtained from each part.

$$\Delta u_1^m = (G_{11}^T G_{11} + \lambda_1 I)^{-1} G_{11}^T (r_1 - f_{11}) \tag{4}$$

$$\Delta u_2^m = (G_{22}^T G_{22} + \lambda_2 I)^{-1} G_{22}^T (r_2 - f_{22}) \tag{5}$$

As for the decoupled control shown in Figure 2, the predicted temperatures of the sections j step ahead can be written as in Equations (6) and (7). Thus, each of these will have taken the interaction into account in the future while calculating the responses and manipulating variables, thus enabling future decoupling. The input vectors, Δu_1^m and Δu_2^m, are obtained by the matrix solution of Equation (8) by multiplying the right-hand side matrix by the inverse of the coefficient matrix, with the help of an algorithm set up in the MATLAB. Then the responses are read after applying the first terms to the process.

$$y_1(t+j) = G_{j,11}\Delta u_1^m(t+j-1) + f_{j,11} + G_{j,12}\Delta u_2^m(t+j-1) + f_{j,12} \tag{6}$$

$$y_2(t+j) = G_{j,21}\Delta u_1^m(t+j-1) + f_{j,21} + G_{j,22}\Delta u_2^m(t+j-1) + f_{j,22} \tag{7}$$

$$\begin{bmatrix} \Phi_1 & \Phi_2 \\ \Phi_3 & \Phi_4 \end{bmatrix} \begin{bmatrix} \Delta u_1^m(t+j-1) \\ \Delta u_2^m(t+j-1) \end{bmatrix} = \begin{bmatrix} \Gamma_1 \\ \Gamma_2 \end{bmatrix} \tag{8}$$

where,

$$\Phi_1 = G_{11}^T G_{11} + \lambda_1 I\,,\ \Phi_2 = G_{11}^T G_{12}$$

$$\Phi_3 = G_{22}^T G_{21}\,,\ \Phi_4 = G_{22}^T G_{22} + \lambda_2 I$$

$$\Gamma_1 = G_{11}^T (r_1 - f_{11} - f_{12})\,,\ \Gamma_2 = G_{22}^T (r_2 - f_{21} - f_{22})$$

After applying the input and reading the response in each of the control mechanisms mentioned above, the calculation is repeated for the next control step and continues cyclically, if possible, until the setpoint is reached. The control gain remains constant during applications and only the f and r vectors are calculated at each sampling interval.

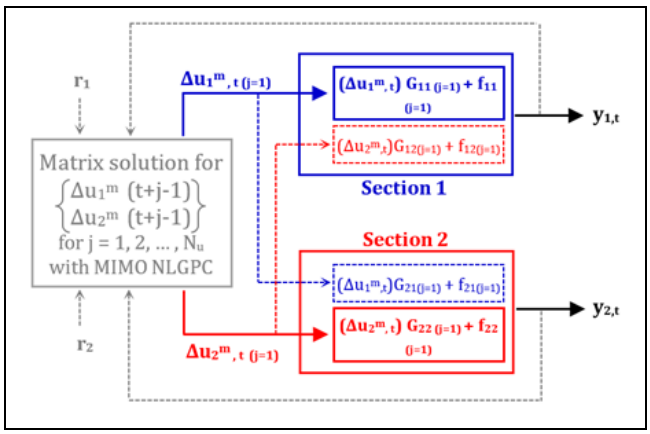

Figure 2. Flow diagram of the decoupled MIMO NLGPC.

In terms of control with discrete-time PID, the response and input based on the ARX model can be defined as in Equations (9) and (10), where G is B/A and A, B and S are polynomials.

$$y(t) = G(z^{-1})\, u(t-1) \tag{9}$$

$$u(t) = \frac{S}{\Delta}[r(t) - y(t)] \tag{10}$$

In the control with SISO PID, the input Equation (10) is applied to the relevant region and the temperature is read from the system. As for the control with MIMO PID, presented in Figure 3, the input values to be applied to the process are obtained with the help of Equations (11) and (12) for the non-decoupled one.

$$u_1(t) = \frac{S_1}{\Delta}[r_1(t) - y_1(t)] \tag{11}$$

$$u_2(t) = \frac{S_2}{\Delta}[r_2(t) - y_2(t)] \tag{12}$$

Regarding the decoupling, the outputs y_1 and y_2 at time t can be defined by Equations (13) and (14). Initially u_1 and u_2 are calculated with Equations (11) and (12). Before they are applied to the process, the inputs are revised as the following, $\{u_1(t) - [u_2(t)G_{12}(z^{-1})/G_{11}(z^{-1})]\}$,$\{u_2(t) - [u_1(t)G_{21}(z^{-1})/G_{22}(z^{-1})]\}$. After the response is read from the process, the calculation is made for the next control step and if

possible, this process is continued cyclically until the response reaches the setpoint.

$$y_1(t) = G_{11}(z^{-1})[u_1(t-1) + T_2u_2(t-1)] + G_{12}(z^{-1})[u_2(t-1) + T_1u_1(t-1)] \quad (13)$$

$$y_2(t) = G_{22}(z^{-1})[u_2(t-1) + T_1u_1(t-1)] + G_{21}(z^{-1})[u_1(t-1) + T_2u_2(t-1)] \quad (14)$$

where,

$$T_1 = -[G_{21}(z^{-1})/G_{22}(z^{-1})], \quad T_2 = -[G_{12}(z^{-1})/G_{11}(z^{-1})]$$

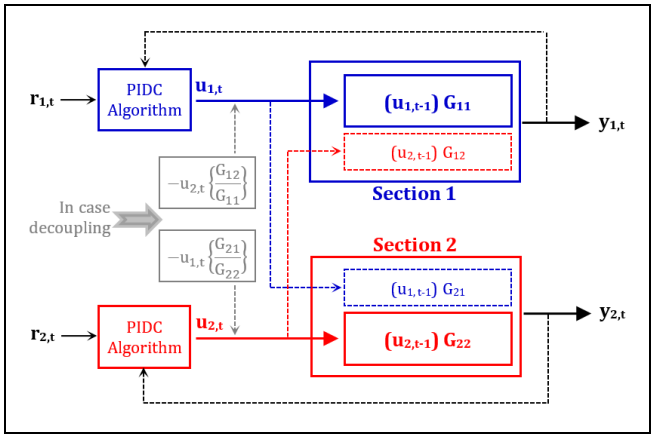

Figure 3. Flow diagram of the control action with MIMO PID.

Regarding the parameters used in the models, they were determined with the help of the PRBS effect and the programs, which were created with the "rarmax" and "arx" tools in MATLAB. In the program, developed with the 'rarmax' tool, ΔA and ΔB were taken as basis instead of A and B polynomials in order to take into account the integral effect of the ARIMAX model. Regression based on curve fitting of models with experimental responses was evaluated according to IAE and ISE. The coefficients of the polynomials E_j, F_j, H_j and G_j were calculated with the algorithms developed in MATLAB. To do this, first, the C polynomial was divided by ΔA up to the number of N_u steps, and from the quotient and remainder, obtained in each division step, the polynomials E_j and F_j were obtained for the jth step, respectively. Then, the polynomial, obtained from the product of E_j and B at each step j, was divided by C, and the polynomials G_j and H_j were obtained for step j from the quotient and remainder, in turn. The optimum values of λ, K_C, τ_I and τ_D were ascertained depending on the rise time, settling time, size of the error, and oscillation frequency.

3 Results of simulation with HYSYS

The effects of reflux ratio, mole ratio and reboiler heat duty on biodiesel mole fraction were investigated earlier in [33] (see Figure 4). In order to understand the effects of all parameters on temperature and biodiesel mole fractions simultaneously, simulation was performed with Aspen HYSYS 8.0 for five parameters and the results were presented in Figures 5 and 6.

When the figures are examined, it is noticed that the temperature and mole fraction profiles are remarkably similar. In other words, the change of the profiles in the column and the reboiler is similar to the change of the parameter values in the operating range. In general, there is a rise in temperature and mole fraction at the reboiler as the heat duty increases and the reflux ratio, feed flow rate, and mole ratio decrease. As to the profiles in the column, the steady-state curves have a significant diminishing as the mole ratio and heat duty get bigger, and a slight lessening when the reflux ratio raises, and a correspondingly significant rising as the flow rate increases. Consequently, feed flow rate, reboiler heat duty and molar ratio have a significant effect on both sides. However, as shown in Figure 6, the variation of the feed inlet temperature in the range of 40–60 °C has no significant influence on them. Supportingly, similar results have been found in the literature. Likewise, the feed inlet temperature was not taken place in the model [35]. Accordingly, the most important parameter affecting the FAME mole fraction is the WCO flow rate, and the other significant one is the mole ratio.

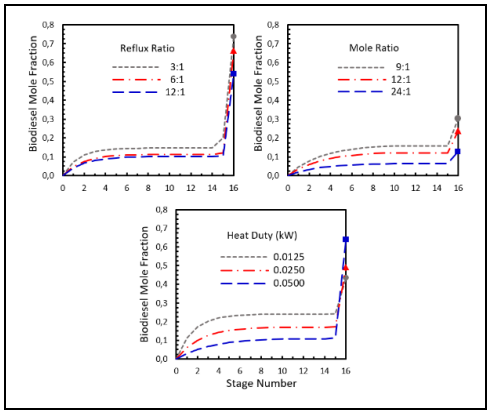

Figure 4. Simulation for the effects of parameters on biodiesel mole fraction [33].

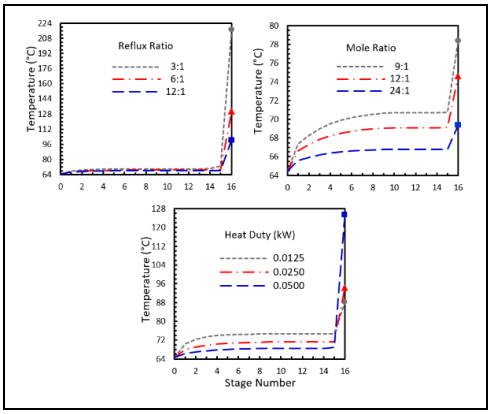

Figure 5. Simulation for the effects of parameters on temperature.

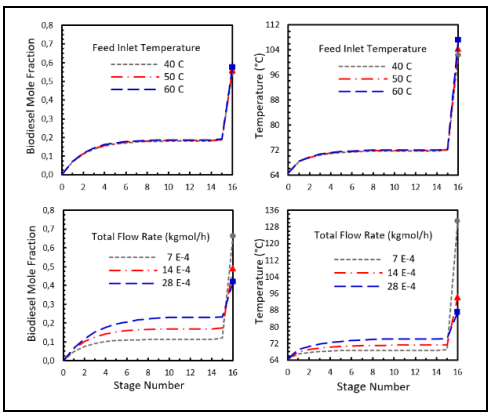

Figure 6. Simulation for the effects of parameters on biodiesel mole fraction and temperature.

Consequently, it has been decided to choose the WCO flow rate and the reboiler heat duty as the manipulating variables to control the temperatures of the reaction and reboiler sides in the experimental control studies, just like in our theoretical control study [32]. Since the feed inlet temperature does not have a significant effect on the temperature and mole fraction profiles in the specified range, the inlet temperature has been taken as 55 °C in the studies. Furthermore, since the continuous circulation of excess methanol in the reaction section is desired, the reflux ratio, which is previously known to have a lower effect on both profiles, has been eliminated. Thus, the excess of methanol evaporates from the reboiler, liquefies in the condenser and flows back to the column incessantly. In this way, it will be ensured that there is always excess methanol in the reaction and that the equilibrium reaction would shift towards the product side. Lastly, the inlet mole ratio has been kept constant as 8.19 [35] in all experimental control studies.

Cosidering what has been said so far, the flowcharts of the RD column process where reaction and reboiler temperatures are controlled by the feed flow rate and heat duty manipulating variables for NLGPC can be illustrated as in Figures 7-9.

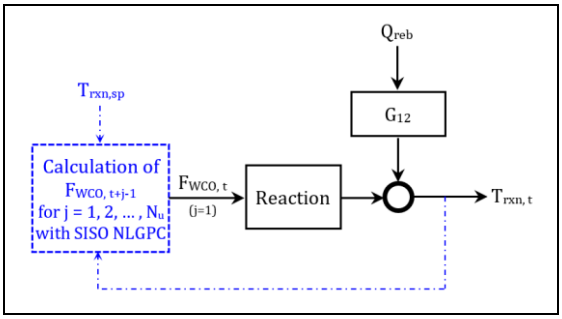

Figure 7. SISO control strategy with NLGPC for the reaction.

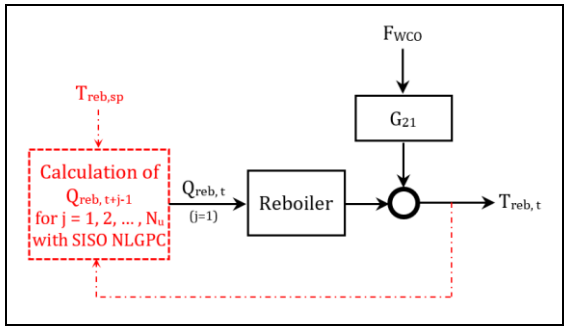

Figure 8. SISO control strategy with NLGPC for the reboiler.

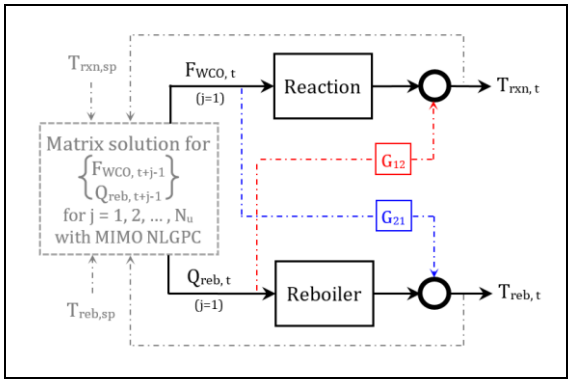

Figure 9. MIMO control strategy with the decoupled NLGPC for reaction and reboiler temperature.

In SISO controls, reboiler heat duty behaves as a load effect in control of the reaction temperature with the help of WCO flow rate as in Figure 7. Similarly, the WCO flow rate has a load effect in controlling of the reboiler temperature with the reboiler heat duty as in Figure 8. In the MIMO control, shown in Figure 9, the WCO flow rate and reboiler heat duty have simultaneously had the inevitable disruptive effect in the region where each does not act as a controller.

4 Implementation of control system

4.1 Results of experimental SISO control

In the experimental studies for SISO control of reaction and reboiler temperatures with WCO flow rate and heat duty, each obtained temperature responses of the reaction and reboiler were presented in Figures 10-13. With respect to the control of reaction temperature with the SISO NLGPC, shown in Figure 10, a setpoint change was applied to see how the course of the reference trajectory and the response behavior would be in the long run. The settling time of the first step was obtained as nearly 550 sec. The following rise time in response to setpoint change was roughly 550 sec. It converged to the setpoint with a slight overshoot and an additional 1250 sec to settle, showing some degree of oscillatory behavior but good reference trajectory tracking. As for the control of the reboiler temperature with SISO NLGPC, the rise time was obtained from Figure 11 as nearly 460 sec. It approached the setpoint with some overshoot, oscillation, and offset over the time followed.

Concerning SISO PID control, settling time of the reaction, shown in Figure 12, were obtained as nearly 840 sec, without any oscillation or offset. In the temperature control of the reboiler, the rise and settling time were found to be almost 485 and 900 sec with a concave curve about half the extent of the step effect in the initial region of the profile followed by a significant overshoot, and an oscillatory response (see Figure 13).

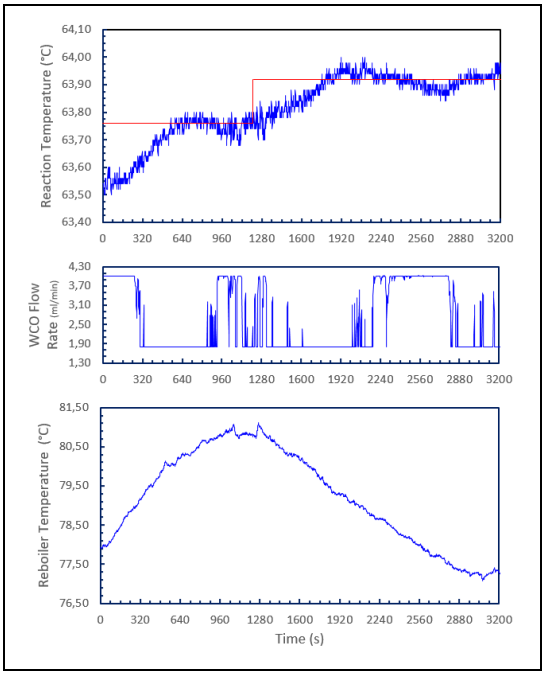

Figure 10. Reaction temperature control by F_{WCO} in SISO NLGPC (T_{rxn_sp1} : 63.76 °C, T_{rxn_sp2} : 63.92 °C, Q_{reb} : 350 W).

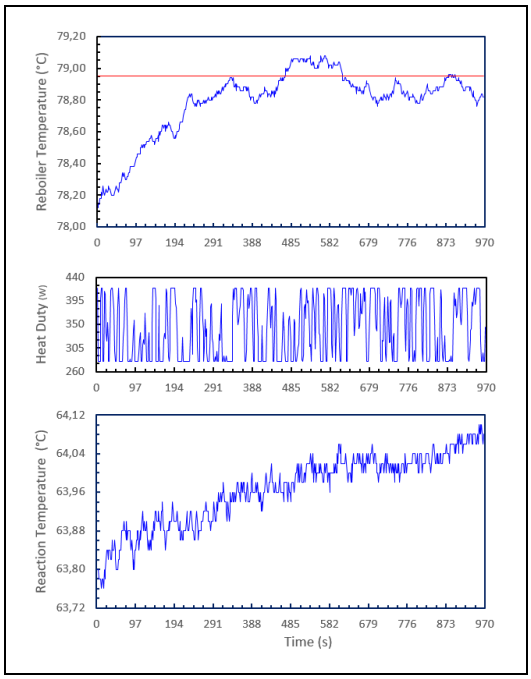

Figure 11. Reboiler temperature control by Q_{reb} in SISO NLGPC (T_{reb_sp} : 78.95 °C, F_{WCO} : 3 ml/min).

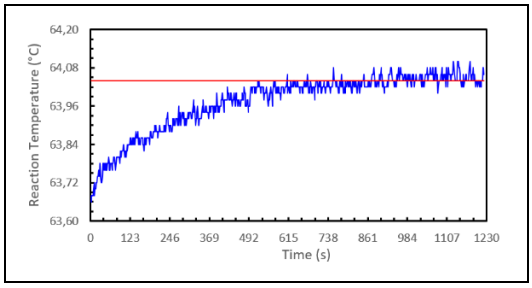

Figure 12. Reaction temperature responses in SISO PID control by F_{WCO} (T_{rxn_sp} : 64.04 °C, Q_{reb} : 350 W).

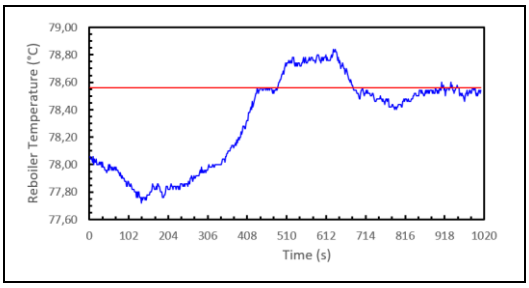

Figure 13. Reboiler temperature responses in SISO PID control by Q_{reb} (T_{reb_sp} : 78.56 °C, F_{WCO} : 3 ml/min).

In terms of free responses in Figures 10 and 11, there is also a change in uncontrolled region temperatures during the simultaneous change of the manipulating variable trying to bring the temperature of the controlled section to the setpoint. Therefore, it can be understood that each manipulating variable has an effect on both side due to the interaction. Supportingly, interaction has also been encountered earlier in steady-state simulation with the Aspen HYSYS shown in Figures 4-6. It is clear that column hydrodynamics and the reboiler temperature will vary with the flow rate at a constant heat duty. Accordingly, the mole ratio in the reaction will vary depending on the amount of methanol that evaporates from the reboiler and flows back fully to the column after condensation. Eventually, these dynamic fluctuations cause complex interaction in mass and heat transfer and equilibrium reaction. Similar situations can occur when the heat duty is changed at a constant flow rate.

Consequently, looking at Figures 10-13 as a whole, it was observed that significant responses were obtained from each controlled region in the SISO experiments where the control of the reaction temperature with the WCO flow rate and the control of the reboiler temperature with the reboiler heat duty were aimed. Namely, each response profile individually converged to its setpoint. Thus, it has been evaluated that each region can be controlled separately by using the manipulating variable specified for it. However, it should not be forgotten that there is also a temperature variation in the uncontrolled section due to the interaction in the system.

4.2 Results of experimental MIMO control

In multivariable control experiments, temperature responses and manipulating variable change, obtained from simultaneous control of reaction and reboiler with non-decoupled and decoupled MIMO NLGPC, were given in Figures 14 and 15.

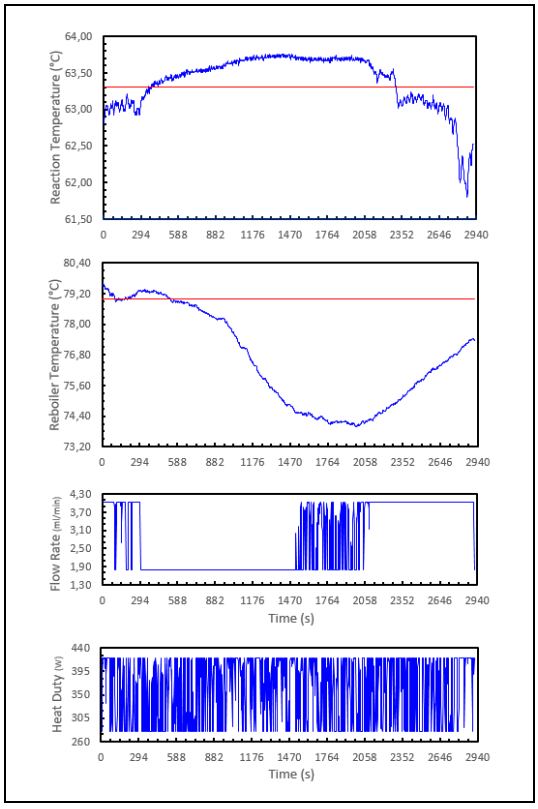

Figure 14. MIMO control by F_{WCO} and Q_{reb} using non-decoupled NLGPC (T_{rxn_sp} : 63.3 °C, T_{reb_sp} : 79.0 °C).

Examining Figure 14, it was noticed that the setpoints could not be reached in the non-decoupled MIMO NLGPC system. Likewise, similar results were previously encountered in our theoretical study [32]. It was observed that the rise time could be obtained around 365 and 90 sec as the lowest values in all experimental cases, and the responses exhibited good control behavior for the reaction and reboiler side in the first 560 and 625 sec, respectively. After these points, the harsh interaction started to dominate the process response, and each profile diverged with oscillation due to strong interaction in non-decoupled MIMO NLGPC.

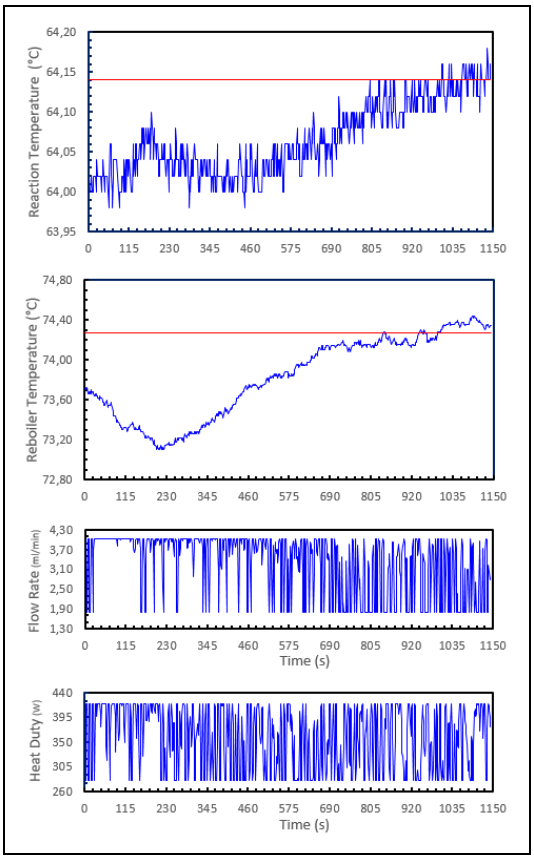

Figure 15. MIMO control by F_{WCO} and Q_{reb} using decoupled NLGPC (T_{rxn_sp} : 64.14 °C, T_{reb_sp} : 74.27 °C).

Although it could not possible to control the temperatures concurrently with the non-decoupled one, it was observed in Figure 15 that they converged to the desired setpoints with the decoupled MIMO NLGPC. The settling time can be taken as 1060 and 1000 sec for the reaction and reboiler side, in turn. The responses converged to the setpoints without oscillation, after both a peak of half the step effect size in the reaction region and a minimum in the step effect size in the reboiler side, which appeared in the initial region of the profiles. However, a slight overshoot was observed in the reboiler response due to some disruptive effects.

In terms of control with MIMO PID algorithms, the response profiles of non-decoupled and decoupled ones were presented in Figures 16 and 17. Seemingly, they are finally approaching their setpoint. However, as shown in Figure 16, due to the vigorous interaction in the non-decoupled MIMO PID control, an offset on both side and an oscillatory behavior with a step effect size peak in the initial area of the reboiler temperature profile were observed over the time scale followed. As might be expected, such a response can be encountered in PID control of real-time processes.

The rise times of the reaction and reboiler sides were read from Figure 16 as approximately 490 and 525 sec respectively, appearing to be the fastest response among all convergent MIMO algorithms. However, from the course of the figures on both sides, it is obvious that the settling times will be over 1750 sec and the responses might eventually have some offset value. This was the longest time encountered in all convergent MIMO algorithms. It should also be noted that the response on the reboiler side is wholly oscillatory.

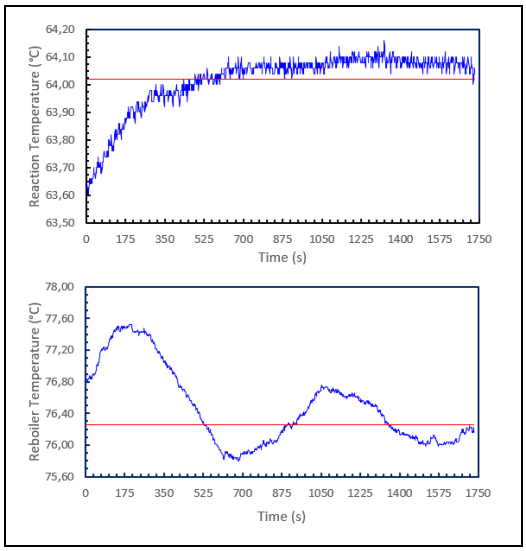

Figure 16. MIMO control by F_{WCO} and Q_{reb} using non-decoupled PID control (T_{rxn_sp} : 64.02 °C, T_{reb_sp} : 76.26 °C).

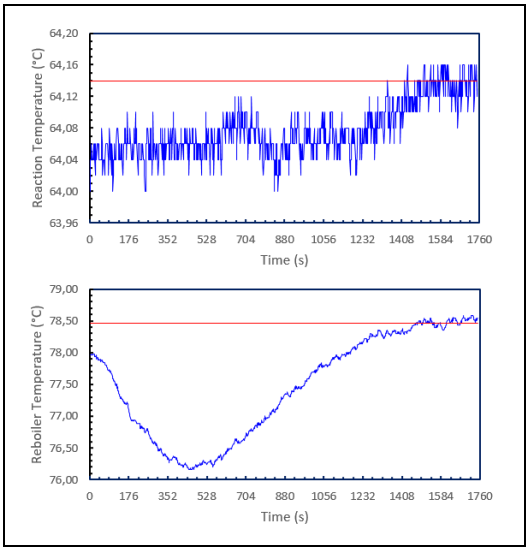

Figure 17. MIMO control by F_{WCO} and Q_{reb} using decoupled PID control (T_{rxn_sp} : 64.14 °C, T_{reb_sp} : 78.46 °C).

Relating to the control with the decoupled MIMO PID shown in Figure 17, the response profiles appeared similar to those obtained with the decoupled MIMO NLGPC. However, unlike them, the settling times of the reaction and reboiler sections, which were determined as 1650 and 1580 sec respectively, were greater. Although some interactions affecting the simultaneous converging response profile were also seen in the decoupled MIMO NLGPC, the responses in decoupled MIMO PID control developed much more sluggish, taking much more time to reach the setpoints in comparison. In particular, the broader and larger concave curve, which is about four times the step effect in the initial region of the reboiler temperature profile, indicates that the interaction in the decoupled MIMO PID control is much more severe than in the decoupled MIMO NLGPC.

Moreover, IAE and ISE have been calculated and presented in Table 1 to contribute to the evaluation of control performances. In non-decoupled MIMO NLGPC these are very huge and, as can be seen from the course of Figure 14, grow larger and larger, supporting the diverging from the setpoints. Among the

converging algorithms included in the study, the values obtained by the reboiler of the decoupled MIMO PID control attracted attention, especially with their larger size. Also, the values obtained from the non-decoupled PID control are greater when compared to the decoupled MIMO NLGPC. Thus, it has been seen once again that the best results are achieved with decoupled MIMO NLGPC.

Table 1. IAE and ISE values obtained from experimental MIMO controls.

Control Method	IAE		ISE	
	T_rxn	T_reb	T_rxn	T_reb
Non–decoup. NLGPC	584.28	4502.02	266.11	17047.12
Decoupled NLGPC	54.22	333.70	5.50	259.41
Non–decoupled PID	83.10	445.40	12.46	315.76
Decoupled PID	70.38	1098.99	5.64	1792.00

To summarize, it has been evaluated that the temperature responses of the reaction and reboiler can converge to the setpoints in all control mechanisms except non-decoupled MIMO NLGPC due to harsh interaction. Among the converging profiles, an offset and oscillation with longer settling time was obtained in the non-decoupled MIMO PID control, and a much sluggish response profile was observed in the decoupled MIMO PID control. As a result, there is particularly good convergence and control performance in the decoupled MIMO NLGPC in all experimental cases examined, in terms of less severe interaction, smaller settling time with no oscillatory behavior, and lower IAE and ISE values. Like our previous theoretical control study [32], the best results and control performance have been achieved in decoupled MIMO NLGPC in all theoretical cases related to non-decoupled and decoupled MIMO NLGPC and PID control.

Upon evaluating the control actions in Figures 10–17, they seem to be aggressive, and the tuning action may need improvement to protect control devices such as peristaltic pumps and mantle heater. In the study, no restrictions were defined as limit values for the manipulating variables in the developed programs. Then, during the calculation of the inputs at each control step, the reference trajectory values were assumed to be equal to the setpoints. Apart from these, while determining the control constants, attention was paid to ensure that the process responds as quickly as possible without oscillation and offset under defined conditions. Thus, the values of manipulating variables to be applied to the process in the next control step were calculated under these circumstances. In other words, in all control studies, in both NLGPC and PID algorithms, when the manipulating variable calculated for the next control step in each control period was outside the specified operating range, the maximum or minimum operating value was assigned to the manipulating variable and applied to the process for that control step. As a suggestion, a reference trajectory function could be developed including a controlled output and a tunable parameter, taking a value between 0 and 1. Additionally, control constants can be tuned to give desired performances by trial-and-error methods. Furthermore, a new codes can be developed that takes into account the lower and upper limit values of the manipulated variables in the calculation steps.

5 Conclusion

In this study, the reaction and reboiler temperature control of the continuous flow, full methanol-recycled and CaO-catalyzed RD column process in biodiesel synthesis from WCO and methanol with non-decoupled and decoupled NLGPC and discrete-time PID were investigated.

Before proceeding to the control studies, the process was simulated with Aspen HYSYS to see the effects of feed inlet temperature, feed flow rate, mole ratio, reflux ratio and reboiler heat duty on temperature responses and FAME mole fraction. It was concluded that the simulation results were compatible with [35] in terms of the effect of the parameters. Accordingly, the most important parameters were determined as feed flow rate, mole ratio and reboiler heat duty. So, WCO flow rate with constant molar ratio and reboiler heat duty were chosen as manipulating variables. As a result of their use in the experiments for temperature control with SISO algorithm in the relevant region, it was observed that the reaction and reboiler temperatures approached the setpoints well, and good responses were obtained.

Consequently, in the light of the information evaluated so far, it can be concluded that the temperature control of the reaction and reboiler of the RD column process can be achieved by all proposed mechanisms, except for the non-decoupled MIMO NLGPC. All in all, it can be emphasized that multivariable control action can be well achieved with decoupled MIMO NLGPC since less severe interaction, lower settling time with no oscillation and lower IAE and ISE.

Lastly, an inspection of controlling the concentration and/or conversion of FAME in terms of temperature can be presented as a suggestion for further research once the correlation between them has been determined.

6 Author contribution statements

In the scope of this study, Mehmet Tuncay ÇAĞATAY in the conceptualization, investigation, methodology, visualization, software, writing-original draft preparation, reviewing and editing; Süleyman KARACAN in the conceptualization, data curation, methodology, supervision, validation, writing-review and editing were contributed.

7 Ethics committee approval and conflict of interest statement

There is no need to obtain permission from the ethics committee for the article prepared. There is no conflict of interest with any person/institution in the article prepared.

8 References

[1] Goli J, Sahu O. “Development of heterogeneous alkali catalyst from waste chicken eggshell for biodiesel production”. *Renewable Energy,* 128, 142-154, 2018.

[2] Thokchom SS, Tikendra NV. “An assessment study of using Turel Kongreng (river mussels) as a source of heterogeneous catalyst for biofuel production”. *Biocatalysis and Agricultural Biotechnology,* 20, 1-5, 2019.

[3] Fonseca JM, Teleken JG, de Cinque Almeida V, da Silva C. “Biodiesel from waste frying oils: methods of production and purification”. *Energy Conversion and Management,* 184, 205-218, 2019.

[4] Milano J, Ong HC, Masjuki HH, Silitonga AS, Chen WH, Kusumo F, Dharma S, Sebayang AH. “Optimization of biodiesel production by microwave irradiation–assisted transesterification for waste cooking oil Calophyllum inophyllum oil via response surface methodology”. *Energy Conversion and Management,* 158, 400-415, 2018.

[5] Ruhul AM, Kalam MA, Masjuki HH, Fattah İR, Reham SS, Rashed MM. "State of the art of biodiesel production processes: a review of the heterogeneous catalyst". *RSC Advances,* 5, 101023-101044, 2015.
[6] Boey PL, Maniam GP, Hamid SA. "Performance of calcium oxide as a heterogeneous catalyst in biodiesel production: a review". *Chemical Engineering Journal,* 168, 15-22, 2011.
[7] Ling JSJ, Tan YH, Mubarak NM, Kansedo J, Saptoro A, Nolasco–Hipolito C. "A review of heterogeneous calcium oxide–based catalyst from waste for biodiesel synthesis". *SN Applied Sciences,* 1, 810, 2019.
[8] Pradana YS, Hidayat A, Prasetya A, Budiman A. "Biodiesel production in a reactive distillation column catalyzed by heterogeneous potassium catalyst". *Energy Procedia,* 143, 742-747, 2017.
[9] Talebian–Kiakalaieh A, Amin NAS, Mazaheri H. "A review on novel processes of biodiesel production from waste cooking oil". *Applied Energy,* 104, 683-710, 2013.
[10] Wang J, Ge X, Wang Z, Jin Y. "Experimental studies on the catalytic distillation for hydrolysis of methyl acetate". *Chemical Engineering & Technology,* 24, 155-159, 2001.
[11] Alaei HK, Salahshoor K, Alaei HK. "Model predictive control of distillation column based recursive parameter estimation method using HYSYS simulation". *International Conference on Intelligent Computing and Cognitive Informatics*, Kuala Lumpur, Malaysia, 22-23 June 2010.
[12] Cong L, Liu X, Zhou Y, Sun Y. "Generalized generic model control of high-purity internal thermally coupled distillation column based on nonlinear wave theory". *AIChE Journal,* 59, 4133-4141, 2013.
[13] Liu X, Cong L, Zhou Y. "Nonlinear model predictive control based on wave model of high-purity internal thermally coupled distillation columns". *Industrial & Engineering Chemistry Research*, 52, 6470-6479, 2013.
[14] Regalado-Méndez A, Romero R, Natividad R, Skogestad S. "Plant-wide control of a reactive distillation column on biodiesel production". *In Computer Science On–line Conference*, Springer, Cham, 27-30 April 2016.
[15] Cheng Y, Chen Z, Sun M, Sun Q. "Active disturbance rejection generalized predictive control for a high purity distillation column process with time delay". *The Canadian Journal of Chemical Engineering,* 97, 2941-2951, 2019.
[16] Giwa SO, Adeyi AA, Giwa A. "Application of model predictive control to renewable energy development via reactive distillation process". *International Journal of Engineering Research in Africa,* 27, 95-110, 2016.
[17] Wu S. "Multivariable PID control using improved state space model predictive control optimization". *Industrial & Engineering Chemistry Research,* 54, 5505-5513, 2015.
[18] Saravanakumar G, Valarmathi K, Iruthayarajan MW, Srinivasan S. "Lagrangian–based state transition algorithm for tuning multivariable decentralised controller". *International Journal of Advanced Intelligence Paradigms,* 8, 303-317, 2016.
[19] Abraham A, Pappa N, Priya MS, Mary Hexy M. "Predictive control design for a MIMO multivariable process using order reduction techniques". *International Journal of Modelling and Simulation,* 37, 199-207, 2017.
[20] Hadian M, Mehrshadian M, Karami M, Makvand AB. "Event–based neural network predictive controller application for a distillation column". *Asian Journal of Control*, 23, 811-823, 2021.
[21] Shin Y, Smith R, Hwang S. "Development of model predictive control system using an artificial neural network: A case study with a distillation column". *Journal of Cleaner Production,* 277, 1-14, 2020.
[22] Cheng Y, Chen Z, Sun M, Sun Q. "Decoupling control of high-purity heat integrated distillation column process via active disturbance rejection control and nonlinear wave theory". *Transactions of the Institute of Measurement and Control,* 42, 2221-2233, 2020.
[23] Karacan S, Hapoğlu H, Alpbaz M. "Application of optimal adaptive generalized predictive control to a packed distillation column". *Chemical Engineering Journal,* 84, 389-396,2001.
[24] Hapoglu H, Karacan S, Koca ZE, Alpbaz M. "Parametric and nonparametric model–based control of a packed distillation column". *Chemical Engineering and Processing: Process Intensification,* 40, 537-544, 2001.
[25] Karacan S. "Application of a nonlinear long range predictive control to a packed distillation column". *Chemical Engineering and Processing: Process Intensification,* 42, 943-953, 2003.
[26] Mahfouf M, Abbod MF, Linkens DA. "Multivariable adaptive fuzzy TSK model–based predictive control with feedforward". *European Control Conference (ECC) IEEE*, Porto, Portugal, 4-7 September 2001.
[27] Karacan S, Hapoğlu H, Alpbaz M. "Multivariable system identification and generic model control of a laboratory scale packed distillation column". *Applied Thermal Engineering,* 27, 1017-1028, 2007.
[28] Marangoni C, Teleken JG, Werle LO, Machado RA, Bolzan A. "Multivariable control with adjustment by decoupling using a distributed action approach in a distillation column". *IFAC Proceedings Volumes*, 42, 857-862, 2009.
[29] Liu X, Wang C, Cong L, Ding F. "Adaptive generalised predictive control of high purity internal thermally coupled distillation column". *The Canadian Journal of Chemical Engineering,* 90, 420-428, 2012.
[30] Haßkerl D, Lindscheid C, Subramanian S, Markert S, Górak A, Engell S. "Dynamic performance optimization of a pilot-scale reactive distillation process by economics optimizing control". *Industrial & Engineering Chemistry Research,* 57, 12165-12181, 2018.
[31] Yadav ES, Indiran T, Priya SS. "System identification and conditional control for an optimal operation of a pilot plant binary distillation column". *International Journal of Computing and Digital Systems,* 9, 139-146, 2020.
[32] Çağatay MT, Karacan S. "Multivariable generalized predictive control of reactive distillation column process for biodiesel production". *Turkish Journal of Engineering,* 6, 40-53, 2022.
[33] Karacan S, Çağatay MT. "Transesterification of waste cooking oil into biodiesel using Aspen HYSYS". *International Journal of Scientific Research in Science and Technology,* 3, 83-87, 2017.
[34] Karacan S, Çağatay MT. "Simulation and optimization of reactive packed distillation column for biodiesel production using heterogeneous catalyst". *International Journal of Energy Applications and Technologies,* 5, 153-160, 2018.
[35] Çağatay MT, Çağatay Ş, Karacan S. "Optimisation of biodiesel synthesis from waste cooking oil in the reactive distillation column using Taguchi methodology". *Journal of Polytechnic,* 24, 175-186, 2021.